



ELSEVIER

Journal of Nuclear Materials 295 (2001) 73–82

Journal of  
nuclear  
materials

www.elsevier.nl/locate/jnucmat

# Pore migration in $\text{UO}_2$ and grain growth kinetics

L. Bourgeois, Ph. Dehautd<sup>\*</sup>, C. Lemaignan, J.P. Fredric

Commissariat à l'Énergie Atomique, Département d'Étude des Combustibles, CEA Grenoble, 17 rue des Martyrs, 38054 Grenoble cedex 9, France

Received 17 October 2000; accepted 22 January 2001

## Abstract

Grain growth and density increase of  $\text{UO}_2$  has been measured during annealings at temperatures between 1650°C and 1750°C, for up to 300 h. The results have been compared to what can be deduced from a review of grain growth kinetics for undoped uranium dioxide. Although much theoretical and experimental work has been devoted to this topic, the mechanism controlling grain boundary migration cannot be clearly identified on the basis of available data. Since grain growth kinetics cannot be separated from pore migration, pore migration rates have been calculated using existing data for  $\text{UO}_2$  mass transport. In the temperature and pore size ranges investigated, it seems that surface diffusion is a more efficient mechanism for pore migration than evaporation–condensation (EC), although these results are strongly dependent on the reliability of the surface diffusion data. © 2001 Elsevier Science B.V. All rights reserved.

## Résumé

On a mesuré la croissance de grain et l'augmentation de la densité de l' $\text{UO}_2$  lors de recuits réalisés entre 1650°C et 1750°C, pour des durées atteignant 300 h. Les résultats sont comparés à ceux déduits d'une revue des cinétiques de croissance cristalline pour le dioxyde d'uranium pur. En dépit d'un important travail aussi bien théorique qu'expérimental déjà disponible sur ce sujet, l'analyse des données ne permet pas d'identifier de façon formelle un mécanisme contrôlant le déplacement des joints de grains. Les cinétiques de croissance cristalline ne peuvent pas être séparées de la migration des pores. Des calculs de vitesses de déplacement des pores sont présentés à partir des données existantes. Dans les gammes de températures et de tailles de pores étudiées, il semblerait que la diffusion de surface soit un mécanisme plus efficace de migration des pores que l'évaporation–condensation, même si les résultats présentés dépendent fortement de la validité des données de diffusion de surface utilisées. © 2001 Elsevier Science B.V. All rights reserved.

## 1. Introduction

In order to achieve increases in burnups in PWRs, it is necessary to control the fission gas release in the fuel rods. With this in mind, the processing of 'coarse grain' microstructures was considered as early as the 1970's, with the aim of reducing the fraction of gas released by increasing the diffusion distances to the grain boundaries. Positive results were reported for coarse-grained  $\text{UO}_2$ , obtained by annealing [1] or by the addition of

$\text{Nb}_2\text{O}_5$  [2] or  $\text{MgO}$  [3]. In the latter case, it would appear that the magnesia precipitates played a role as significant as grain size only by acting as heterogeneous nucleation sites for fission gas and thereby pinning a large volume of intragranular gas. In the case of coarse-grained microstructures, it was decided first of all to examine  $\text{UO}_2$  grain growth.

Nuclear fuel based on  $\text{UO}_2$  or  $(\text{U}, \text{Pu})\text{O}_2$  is processed by powder sintering. Grain growth in the final stage of sintering is the result of interactions between the grain boundaries and the residual porosity. The aim of this study is therefore to examine pure, stoichiometric  $\text{UO}_2$  grain growth kinetics as well as pore migration rates controlled either by surface diffusion or by vapor phase transport in the pores. The reasons for the uncertainty

<sup>\*</sup> Corresponding author.

E-mail address: dehautd@cea.fr (Ph. Dehautd).

concerning the identification of the mechanism controlling grain boundary motion will be discussed.

## 2. UO<sub>2</sub> grain growth

Several studies have been performed in the last decades, but a general review of the mechanisms proposed is lacking. In the following section major results and approaches are presented, in order to provide basis for the discussion of the results obtained.

### 2.1. Analytical models

The first kinetic model developed by Burke and Turnbull [4] was based on the assumption that mobility and surface energy were the same for all grains and that driving force was inversely proportional to grain size. In this case, grain growth in isothermal conditions should follow the relationship:

$$\overline{G^2}(t) - \overline{G_0^2} = k(T) \cdot t \quad \text{with } k(T) = \frac{k}{T} \exp\left(\frac{-Q}{RT}\right),$$

where  $G_0$  is the average grain size of the sample before annealing,  $G(t)$  is the average grain size after an annealing time  $t$  at a temperature  $T$ ,  $k$  is a constant and  $Q$  is the activation energy of the mechanism controlling grain boundary motion. In a restricted temperature range,  $k/T$  can be assimilated to a constant  $k_0$ . This equation should be applicable to dense, undoped materials, but in fact it has rarely been observed, even on high-purity metals obtained by zone melting [5].

From these first experiments, a whole series of theories has been developed with equations of the following type:

$$\overline{G^n}(t) - \overline{G_0^n} = k(T) \cdot t.$$

In the case of ceramic materials such as UO<sub>2</sub>, a large proportion of the porosity is located at the grain boundaries. The pinning properties of these pores were taken into account for the first time by Kingery and François [6]. For a particular microstructural development, sometimes called solarisation, they observed that grain growth and pore growth took place at a practically constant density. The ratio between the average size of the pores and that of the grains remained constant, with pore growth taking place through coalescence when the pores migrated with the grain boundaries. In such conditions, an exponent  $n = 3$  for the above equation was more appropriate than the exponent  $n = 2$  to describe grain development (and pore development). Nichols [7] extended this analysis to the case of boundary movement controlled by the pores. Based on the product of mobility by the force for pore migration rates, Nichols obtained exponents  $n = 3, 4$  and  $5$  for grain growth ki-

Table 1

Normal grain growth exponent  $n$  when grain boundary movement is controlled by pore migration (from Nichols [7] and Brook [8]): EC = evaporation condensation

$n$	Pore migration mechanism	
	Nichols [7]	Brook [8]
2	–	EC at $P = 2\gamma/r$
3	EC at $P = 2\gamma/r$	EC at $P = c^{st}$ or lattice diffusion
4	EC at $P = c^{st}$ or lattice diffusion	Surface diffusion
5	Surface diffusion	–

netics according to the nature of the active mechanism for pore migration (Table 1). Brook [8] also proposed different exponents when grain growth is controlled by pores migration. Pore growth is assumed to take place according to the mechanism described by Kingery and François, considering that grain growth is sufficiently rapid in relation to densification, so that the pore volume fraction remains roughly constant. The experiments conducted by Nichols and Brook did not result in a constant exponent  $n$  for a given mechanism because of a difference in the estimated pinning force exerted by a pore (Table 1).

These various studies were used to explain exponents  $n$  larger than 2. However these studies were limited to specific pore–grain configuration and by restricting the kinetic aspects to the study of the growth of an average grain isolated in a matrix. Subsequently, aspects not taken into account in the first kinetic models, such as grain size distribution, topological constraints within the time development growth of each grain for a given distribution, have been examined. Although these aspects are well known outside the framework of the UO<sub>2</sub> field, computer simulations of normal grain growth have been developed recently: Anderson et al. [5], Srolovitz et al. [9,10] or Weygand et al. [16] used the Monte Carlo method to simulate microstructural development. The experiments carried out by Anderson et al. resulted in an exponent  $n = 2.44$  for pure, dense systems, while exponent  $n = 1.75$  is obtained by Weygand. The difference with the exponent  $n = 2$  given by Burke and Turnbull is explained by the interactions between grain boundaries, or at triple junctions, for example when a small grain disappears.

Changes to the kinetic description have also been suggested. MacEwan and Hayashi [11] used a relationship of the following type:

$$\overline{G^n}(t) - \overline{G_0^n} = k(t) \cdot t^m \quad \text{with } m \neq 1, \quad (1)$$

explaining the deviation from the ideal case (i.e.,  $m = 1$ ) by a reduction in the driving force with time. With this type of equation, the deduced activation energies  $Q$

depend on the value of  $m$  used. This point will be developed below. Burke [12], noting the existence of a critical size for  $\alpha$ -brass grain growth in the presence of stable precipitates, suggested the following growth rate:

$$\frac{d\bar{G}}{dt} = k \left( \frac{1}{\bar{G}} - \frac{a}{\bar{G}_m} \right), \quad (2)$$

where  $\bar{G}_m$  is the upper limit of the grain size and  $k$  and  $a$  are constants. Ainscough et al. [13] measured grain growth between 1573 and 1773 K for annealing times of up to 24 weeks on  $\text{UO}_2$ . Rejecting the exponent  $n = 3$ , on the basis of their results, they applied Eq. (2) to  $\text{UO}_2$  grain growth, in order to take into account the effect of pore pinning, since this equation has been proposed for materials where inclusions pin the grain boundaries. The upper limit of the grain size is then only a function of temperature. Integrating over time, Eq. (2) becomes

$$\bar{G}_m \cdot (\bar{G}_0 - \bar{G}) + \bar{G}_m^2 \cdot \ln \left( \frac{\bar{G}_m - \bar{G}_0}{\bar{G}_m - \bar{G}} \right) = k(T) \cdot t. \quad (3)$$

This representation is not in absolute agreement with other studies conducted at higher temperatures. However, by selecting only the experiments where the O/U ratio is very close to stoichiometry ( $\text{UO}_{2.000 \pm \epsilon}$ ), the kinetic constants  $k(T)$  are within a factor of 4 consistent with the values extrapolated from the data of Ainscough et al. [13].

## 2.2. Data on grain growth kinetics

Table 2 shows the grain growth kinetics observed for  $\text{UO}_2$  in isothermal conditions by various experimenters. Several comments have to be given about these data: Lyons et al. [15] performed a general overview of the early studies by attempting to represent all the data by means of an exponent  $n = 3$ . As discussed above, the reliability of such an approach is however questionable. Considering that the values of  $Q$  obtained in these different experiments varied between 280 and

660  $\text{kJ mol}^{-1}$ , they have proposed a relationship between the constants  $k_0$  and the different activation energies  $Q$ :

$$k_0 = \exp(5.096 + 5.923 \times 10^{-5} \cdot Q) \quad \text{with } Q \text{ in } \text{J mol}^{-1} \quad (4)$$

The results obtained by MacEwan [14], published in the form  $n = 2$  and  $m = 0.8$ , were reinterpreted by MacEwan and Hayashi with  $n = 2.5$  and  $m = 1$ , then by Nichols with  $n = 3$  and  $m = 1$ , which has the effect of increasing the activation energy value from 364 to 456 then 518  $\text{kJ mol}^{-1}$ . The kinetic equation proposed by Olsen [17] is also based on the analysis of four earlier experiments.

If it is assumed that all the tests carried out refer to  $\text{UO}_2$  powders which are pure enough to ignore any impurity induced drainage process, the residual sintering porosity is the only expected limitation to the intrinsic migration rate of the grain boundaries. The exponents  $n$  and the activation energy  $Q$  in Table 2 may be attributed to the basic mechanisms controlling the pore migration: i.e., ion surface diffusion ( $D_s$ ), vacancy bulk diffusion ( $D_v$ ), cation  $\text{U}^{4+}$  self-diffusion or evaporation–condensation (EC). The activation energies of these processes have to be detailed.

Evaporation is essentially congruent for stoichiometric  $\text{UO}_2$  and its sublimation enthalpy can be calculated using the equation proposed by Younes [21] for a temperature range between 1200 and 3120 K:

$$\Delta H_s^0 = 630.14 - 3.85 \times 10^{-2}T + 25.67 \times 10^{-6}T^2 - 7.56 \times 10^{-9}T^3 \quad (\text{in } \text{kJ mol}^{-1}; T \text{ in K}). \quad (5)$$

In the temperature range for industrial sintering and grain growth [1600–2000°C],  $\Delta H_s^0$  is close to 590  $\text{kJ mol}^{-1}$ . For self-diffusion of  $\text{U}^{4+}$ , Knorr et al. [22] gave an overview of the dependence of  $D_v$  on a deviation in stoichiometry,  $x$  of  $\text{UO}_{2+x}$ . The activation energy would be about  $\Delta H_v^0 = 540 \text{ kJ mol}^{-1}$  for stoichiometric

Table 2

Grain growth kinetics published on stoichiometric  $\text{UO}_2$ . Unit of constant  $k_0$  is directly related to the growth exponent  $n$

Authors	Year	$n$	$k_0$ ( $\mu\text{m}^n \text{h}^{-1}$ )	$Q$ ( $\text{kJ mol}^{-1}$ )	$[T$ ( $^\circ\text{C}$ )]	Mechanism of pore migration
MacEwan [14]	1962	2 ( $m=0.8$ )	–	363.7	[1550–2440]	–
Lyons et al. [15]	1963	3	$1.7 \times 10^{10}$ to $2.5 \times 10^{19}$	280–660	[1400–2400]	–
MacEwan and Hayashi [11]	1965	2.5	–	455.6	[1550–2440]	–
Nichols [7]	1966	3	–	518.3	–	EC at $P = 2\gamma/r$
Singh [34]	1977	3	$5.2 \times 10^{14}$	502.9	[1800–2100]	EC at $P = 2\gamma/r$
Olsen [17]	1979	4	$1.72 \times 10^{13}$	386.8	–	EC at $P = c^{\text{st}}$
Soliman et al. [18]	1984	4	$5.5 \times 10^{14}$	449.9	[1600–1900]	EC at $P = c^{\text{st}}$
Glodeanu et al. [19]	1987	4	$1.7 \times 10^{15}$	466.6	[1600–1800]	EC at $P = c^{\text{st}}$
Kogai et al. [20]	1989	4	$3.79 \times 10^{18}$	594.1	[1800–2000]	–

UO<sub>2</sub>, but this value decreases with  $x$  to reach only 420 kJ mol<sup>-1</sup> for UO<sub>2.001</sub>.

The measurements of the surface diffusion coefficient are without doubt the less reliable. They are usually obtained by means of mass transport methods (grain boundary grooving or scratch decay) based on surface relaxation or by means of tracers.

Mass transport methods must be adjusted for the evaporation, which becomes a significant factor above 1400°C, according to Maiya [23] and for the surface energy anisotropy which causes significant faceting and consequently disturbs groove relaxation, as observed by Matzke [24]. The data compiled by Maiya and Matzke from nine different experiments give the following relationship:

$$D_s \text{ (cm}^2 \text{ s}^{-1}\text{)} = 5 \times 10^5 \exp(-450000/RT)$$

with  $1200 < T < 1800^\circ\text{C}$  and  $R$  in  $\text{J mol}^{-1} \text{K}^{-1}$ . (6)

The values of  $D_s$  have been estimated by Matzke to be within an experimental scatter band of two orders of magnitude for the temperature range examined. Significant problems arise with respect to mathematical (and theoretical) processing of the experiments using tracers, as shown in the example reported by Olander [25]. Using the results produced by Marlowe and Kazanoff [26], he arrived at a re-evaluation of  $D_s$  by a factor of  $10^4$  at 1915°C by taking into account various ‘interference’ processes. Zhou and Olander [27] subsequently obtained very high values for  $D_s$ , with a pre-exponential coefficient of  $D_0 \sim 5 \times 10^6 \text{ cm}^2 \text{ s}^{-1}$  and an activation energy of the order of  $360 \pm 60 \text{ kJ mol}^{-1}$ .

It appears thus that the data obtained from these numerous early experiments are not reliable enough to predict the grain size at the large values required for high burnup fuels. In particular, the addition of U<sub>3</sub>O<sub>8</sub> from recycled scrap and waste of manufacturing, often causes porosities which are likely to disturb grain boundary movement, within the limits of the natural migration of these pores. The aim of the present experiments was to analyse uranium dioxide grain growth, with and without the addition of U<sub>3</sub>O<sub>8</sub>, in order to determine reliable kinetic constants, for sintered products obtained from powders prepared by dry conversion.

### 3. Experimental

The UO<sub>2</sub> powder used was produced by a dry conversion process. It contained an organic pore-forming agent. The batches, identified as T0 and T12, contained respectively 0 and 12 wt% of U<sub>3</sub>O<sub>8</sub>. After sintering for 5 h at 1750°C in dry hydrogen, the density values for these batches were 10.64 and 10.51 g cm<sup>-3</sup>, respectively and the grain sizes 10.4 and 8.8 μm. These pellets were annealed in dry hydrogen at 1650°C, 1700°C and 1750°C

for periods of between 12 and 500 h. Temperatures were measured using WRe 5/26 thermocouples. Grain sizes were measured by the linear intercept method on polished, etched sections, using a statistically representative number of grains. The changes in density of the fuel pellets during heat treatment were monitored by hydrostatic weighing in ethanol. Five pellets were weighed for each annealing time. The standard deviations of the densities were between 2 and  $7 \times 10^{-3} \text{ g cm}^{-3}$ .

### 4. Results

Table 3 shows the grain sizes and relative density values (normalised to the theoretical density of 10.96 g cm<sup>-3</sup>) during annealing at 1650°C, 1700°C and 1750°C. During the heat treatments the grain sizes increase and tend to saturate. A fourfold increase in grain size is obtained for the high temperature annealings after 300 h. It should be pointed out that the addition of U<sub>3</sub>O<sub>8</sub> (T12) reduces significantly the density, as expected, with an associated lower grain growth. In Fig. 1, the kinetics of grain growth is reported, for the two batches, while Fig. 2 stresses the different correlations between grain growth and reduction of porosity.

When the annealing time increases, there is a slight densification, though this is limited (<1.2%); this densification is more significant for batch T12, which contained U<sub>3</sub>O<sub>8</sub>. Micrographic examination showed a moderate increase in pore size during annealing. However, the grain boundaries were able to pass across a significant fraction of the pores.

For batch T0, the best fit of the data, according to the formula (1) of MacEwan and Hayashi, is obtained with an exponent  $n = 3$ . The slopes of the logarithmic plots are very close to 1 and the best-fit leads to  $0.958 \leq m \leq 1.074$  (Fig. 3(a)). The constants  $k(T)$  obtained for the different temperatures allow one to have access to the activation energy of the process controlling the grain growth kinetics. The value obtained is then 701 kJ mol<sup>-1</sup> with a kinetic constant of  $k_0 = 5.37 \times 10^{20} \mu\text{m}^3 \text{ h}^{-1}$ . If the slopes are forced to be equal to 1, the new constants  $k(T)$  obtained will then give an activation energy of 529 kJ mol<sup>-1</sup> and a constant  $k_0 = 1.46 \times 10^{16} \mu\text{m}^3 \text{ h}^{-1}$ .

Various adjustment procedures of the results have been tested in order to improve the fitting parameters. The three couples of ( $k_0$ ,  $Q$ ) values obtained for batch T0 are the following:

- by direct fitting:  $k_0 = 5.37 \times 10^{20} \mu\text{m}^3 \text{ h}^{-1}$  and  $Q = 701.1 \text{ kJ mol}^{-1}$ ;
- by fitting without the point (1650°C,  $\bar{G} = 13.4 \mu\text{m}$ ):  $k_0 = 5.08 \times 10^{15} \mu\text{m}^3 \text{ h}^{-1}$  and  $Q = 508 \text{ kJ mol}^{-1}$ ;
- by imposing  $m = 1$ :  $k_0 = 1.46 \times 10^{16} \mu\text{m}^3 \text{ h}^{-1}$  and  $Q = 528.7 \text{ kJ mol}^{-1}$ .

All these values are fairly consistent with the correlation proposed by Lyons et al. as shown in Fig. 4.

Table 3  
Grain size and relative density of the heat-treated fuel pellets

Annealing time (h)	$T = 1650^{\circ}\text{C}$		$T = 1700^{\circ}\text{C}$		$T = 1750^{\circ}\text{C}$	
	Batch T0	Batch T12	Batch T0	Batch T12	Batch T0	Batch T12
<i>Grain size (<math>\mu\text{m}</math>)</i>						
0	10.4	8.8	10.4	8.8	10.4	8.8
12	–	–	–	–	17.7	14.9
24	13.4	11.5	16.7	13.0	–	–
48	–	–	–	–	24.5	19.3
96	20.25	16.0	25.2	19.7	33.5	25.5
192	23.5	18.75	–	–	–	–
300	–	–	–	–	45	32.3
500	33.0	23.0	40.8	30.6	–	–
<i>Relative density (%)</i>						
0	97.11	95.90	97.15	95.89	97.06	95.85
12	–	–	97.33	96.18	97.30	96.21
24	97.31	96.13	97.45	96.31	–	–
48	–	–	97.57	96.54	97.56	96.53
96	97.52	96.57	97.71	96.72	97.63	96.70
192	97.68	96.71	97.84	96.86	–	–
300	–	–	–	–	97.84	97.00
500	97.80	97.01	97.89	97.14	–	–

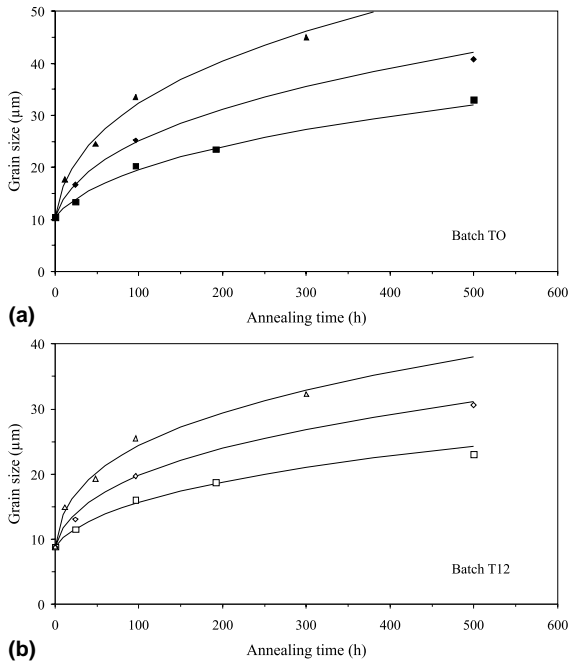


Fig. 1. Grain size as a function of time and temperature during grain growth of stoichiometric  $\text{UO}_2$  samples: (a) batch T0 (■)  $1650^{\circ}\text{C}$ , (◆)  $1700^{\circ}\text{C}$  and (▲)  $1750^{\circ}\text{C}$ ; (b) batch T12 (□)  $1650^{\circ}\text{C}$ , (◇)  $1700^{\circ}\text{C}$  and (△)  $1750^{\circ}\text{C}$ .

For batch T12, the slopes of  $\ln(\overline{G}^n(t) - \overline{G}_0^n)$  as a function of  $\ln t$  are quite different from 1, whether with  $n = 3$  or  $n = 4$ , and also from one temperature to an-

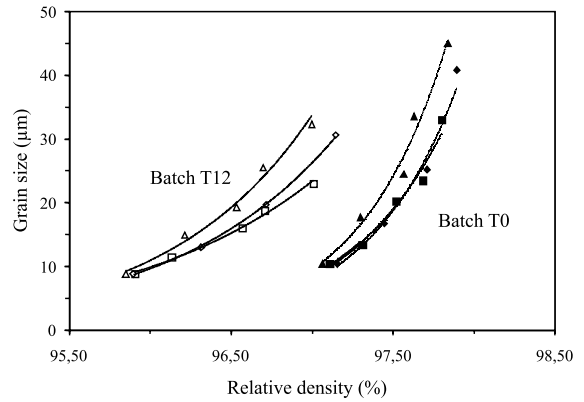


Fig. 2. Variation in grain size as a function of relative density during annealing of batches T0 and T12.

other (Fig. 3(b)). Consequently, there is a weak correlation between the values of  $\ln k(T)$  and  $1/T$ . Therefore, in order to describe grain growth in this batch, it must be assumed that either  $m$  has a value different from 1, or that the exponent  $n$  is not an integer if  $m = 1$  is retained.

### 5. Discussion

For these experiments, a value for  $Q$  of  $701 \text{ kJ mol}^{-1}$  was determined if the aim was simply to find the best possible regression of the experimental points. This value seems high and difficult to compare with the activation energies of the various pore migration

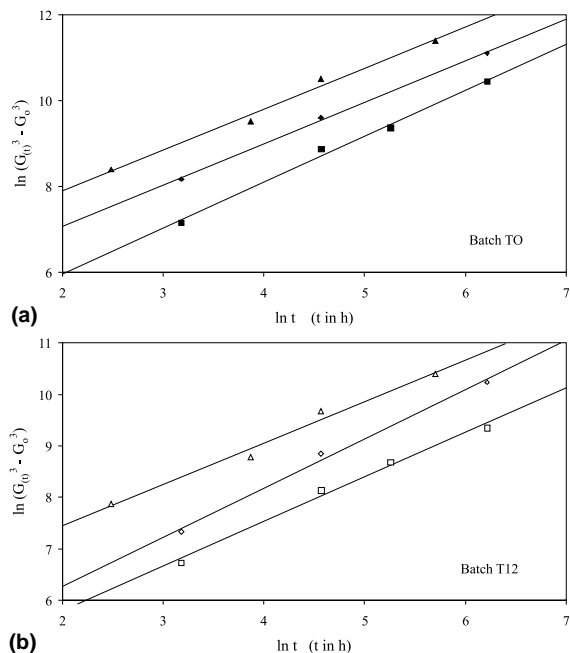


Fig. 3. Variation in grain size with annealing time and temperature: (a) batch T0 (■) 1650°C, (◆) 1700°C and (▲) 1750°C; (b) batch T12 (□) 1650°C, (◇) 1700°C and (△) 1750°C.

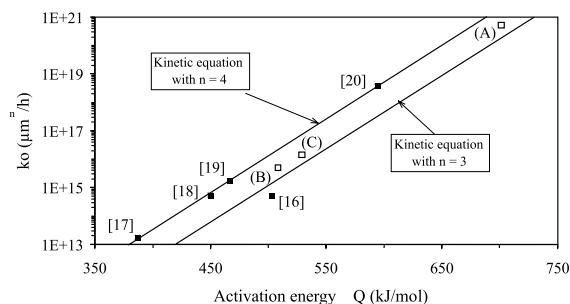


Fig. 4. Relationship between constants  $k_0$  and activation energies  $Q$  from literature data and the present study. With exponent  $n = 3$ , couples ( $k_0$  ( $\mu\text{m}^3 \text{h}^{-1}$ ),  $Q$  ( $\text{kJ mol}^{-1}$ )) are respectively: ( $5.37 \times 10^{20}$ , 701.1) as point (A), ( $5.08 \times 10^{15}$ , 508.2) as point (B) and ( $1.46 \times 10^{16}$ , 528.7) as point (C).

mechanisms, in spite of satisfactory correlation coefficients. By imposing  $m = 1$  or by eliminating a value for the short annealing times, the values obtained for ( $k_0$ ,  $Q$ ) were in-between the value obtained by Glodeanu et al. and those of Kogai et al., but with a different exponent  $n$  (3 for this work, instead of 4 for the others).

Three remarks should be made in relation to the procedure chosen to determine the kinetic constants ( $m \approx 1$ ,  $n = 3$ ,  $k_0$  and  $Q$ ).

(i) The slow grain growth of  $\text{UO}_2$  means that fairly long annealing times are required (at least a hundred hours at 1700°C) in order to obtain grain sizes significantly different from the initial grain size  $\overline{G}_0$ . The number of experimental values is therefore usually limited (typically 5 to 8 samples, including the initial reference). The lack of accuracy caused by this experimental constraints results in fluctuations in the slopes of the  $\ln(\overline{G}^n(t) - \overline{G}_0^n)$  plots as a function of  $\ln t$  when  $n$  is an integer. If slopes of  $m = 1$  are used to fit the experimental points approximately, it is important to understand the limits of such a constrain for obtaining reliable activation energy values, especially when the experimental points seem to deviate significantly from slopes  $m = 1$ , as in the case of T12. If the annealing temperatures are raised, the annealing time can be effectively reduced, but this means working above 2000°C for about 10 h in order to obtain grains in the range of 100  $\mu\text{m}$ .

(ii) The choice of exponent  $n$  is essential for determining the activation energy value. Matzke [28] already drew attention to this point using data obtained by MacEwan and Hayashi [11] at 1832°C. By using equations of the type  $\overline{G}^n(t) - \overline{G}_0^n = k(T) \cdot t^m$ , he observed that the couples ( $n = 2$ ,  $m = 0.77$ ), ( $n = 2.5$ ,  $m = 1$ ), ( $n = 3$ ,  $m = 1$ ) and ( $n = 4$ ,  $m = 1.3$ ) all correctly described the experimental points, which makes it difficult to choose a specific couple. In particular, it does not exist any firm theory to explain a value of  $m \neq 1$ . According to the results of the present study, the couple ( $n = 3$ ,  $m = 0.96$ ) gives an activation energy value of 508  $\text{kJ mol}^{-1}$ . An exponent of  $n = 4$  has also been tested to represent the experimental values and straight lines were in fact obtained, but with slopes of about 1.23 (Fig. 5). The couple ( $k_0$ ,  $Q$ ) thus obtained was  $k_0 = 2.57 \times 10^{20} \mu\text{m}^4 \text{h}^{-1}$  and  $Q = 651 \text{kJ mol}^{-1}$ . If  $m$  values different from 1 are accepted, Fig. 4 shows that, from a strictly numerical point of view, it is impossible to decide between the two values of  $n$ , 3 or 4. However, the choice of exponent  $n$  deter-

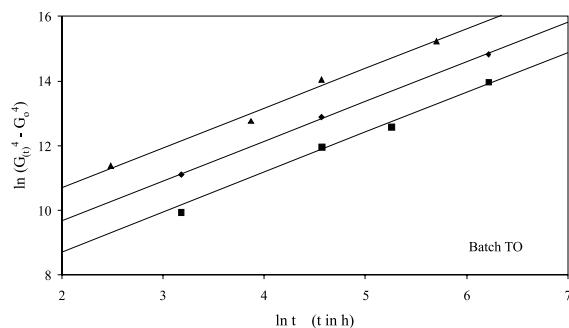


Fig. 5. Grain growth data for batch T0, plotted in a different way. With  $n = 4$ , good fits are possible with time exponent  $m = 1.23$ .

mines the activation energy value. For batch T0, it may appear inappropriate to use a value of  $m = 0.96$  instead of 1. On the other hand, to describe grain growth for batch T12, either a non-integer exponent  $n$  must be used, or a value of  $m \neq 1$  must be accepted if  $n$  is to remain an integer. This behaviour of batch T12 requires a final comment:

(iii) The ‘theoretical’ grain growth exponents were obtained for very precise pore–grain configurations, with the residual sintering pores located at the grain boundaries. For batch T12, a large part of the porosity was caused by the reduction of the recycled  $U_3O_8$  to  $UO_2$ , and this porosity appeared to limit grain boundary movement (Fig. 2). It is likely that the porosity was responsible for the deviation from the theoretical values of  $n$  and  $m$ . Studies on  $UO_2$  are not always conducted under the best conditions for obtaining exponent values,  $n$ , since during annealing, there is some separation from the pores and associated repining sequences. To the authors’ knowledge, there have not been other studies on  $UO_2$ , dealing only with the last stage of sintering, where only stable residual pores remain at the boundaries, as it was the case in the studies carried out, for example, by Zhao and Harmer [29] on alumina.

The interpretation of all the results, including those reported in Table 2, with a concern of pore growth mechanism, raises three main difficulties:

(i) The values  $\Delta H_v^0$  and  $\Delta H_s^0$  are fairly similar.  
(ii) The fuel properties strongly depend on the exact O/U ratio of the condensed phase. Even though the kinetics data given in Table 2 refer to stoichiometric  $UO_2$ , slight variations in  $x$  may not be ruled out in view of the temperature range investigated. While the impact of such variations on the volume diffusion of uranium or on vapour phase composition is well documented, very little is known about the impact on surface diffusion coefficients.

(iii) Last, different interpretations were proposed by Nichols and by Brook for the same value of the exponent  $n$ . The mechanisms proposed by the authors referred to in Table 2 are all based on the work carried out by Nichols. Olsen, Soliman et al. and Glodeanu et al. thus suggested that the boundary motion is controlled by the pores, which migrate by a  $UO_2$  EC mechanism, as deduced from the exponent  $n = 4$ . However, their activation energy values are far from the sublimation enthalpy of  $UO_2$ . According to the exponents established by Brook ( $n = 4$ ), which are more commonly used by authors working on ceramics other than nuclear ceramics, a pore migration mechanism through surface diffusion would be active. The activation energies obtained by Olsen, Soliman et al., as well as Glodeanu et al. are thus very close to the values compiled by Matzke (Eq. (6)). However, it would be unreliable to decide for a given transport mechanism on the sole basis of the activation energies and grain

growth exponents  $n$ , considering  $n$  detail the ways these parameters are obtained.

Indeed, three parameters are involved in grain growth kinetics, namely  $n$ ,  $k_0$  and  $Q$ . Experiments conducted by Lyons et al. show that if one of the parameters is fixed ( $n = 3$ ), a relationship will be established between the two others, transforming the pre-exponential coefficient  $k_0$  into a simple adjustable parameter. The confidence given to the experimental value of  $Q$  then becomes very relative. The results obtained by Singh and those of the present study are compared in Fig. 9. The equation proposed by Lyons et al. would appear to give a correct representation of these recent results for which the kinetic parameter  $n = 3$  is used. Using the results of the references [17–20], and choosing  $n = 4$ , the same kind of relationship is obtained, with an excellent correlation coefficient, leading to

$$k_0 = \exp(5.970 \times 10^{-5} \cdot Q + 7.248). \quad (7)$$

A very good adjustment of  $k_0$  as a function of  $Q$  is confirmed, regardless of the exponent value. With this relationship, the term  $k_0 \exp(-Q/RT) = \exp((5.970 \times 10^{-5} - 1/RT)Q + 7.248)$  can be assimilated to a constant for temperatures close to  $(5.970 \times 10^{-5} R)^{-1}$ , i.e., about 1750°C. In such conditions, the experimental points can be plotted on the basis of very different kinetic laws. Thus, the equations proposed by Soliman et al., Glodeanu et al. and Kogai et al. are virtually identical in the conditions selected in Table 4, despite a variation in activation energies  $Q$  of 150 kJ mol<sup>-1</sup>. Indeed the experimental points obtained by Glodeanu et al. at  $T = 1700^\circ\text{C}$  are better described with the equation proposed by Olsen [17] for grain growth, at least up to 50 h annealing time. Based on the current precision on grain size measurement, the four kinetic equations, represented in Fig. 6, are virtually indistinguishable, even for annealing times of up to 300 h.

In order to consider what could be the effect of the migration rate of the pores on grain growth, this process has to be analysed in more detail. Thus, the relative importance of surface diffusion and vapour phase transport phenomena, have been computed for stoichiometric  $UO_2$  pore migration rates.

## 6. Pore migration rates

Whatever the mechanism of the pore migration, a precise description of their shape under the dragging force of the grain boundary is requested.

Hsueh et al. [30,31] have developed a pore/boundary interaction model, taking into account the dissymmetry of the pore faces for the existence of the pinning force, in the absence of a temperature gradient. The geometrical parameters needed to obtain migration rates according

Table 4

Mass transport parameters used for calculating pore migration rates in stoichiometric  $\text{UO}_2$ 

Density ( $\text{kg m}^{-3}$ )	$\rho$	10960
Molecular weight (kg)	$m$	$4.48 \times 10^{-25}$
Molecular volume ( $\text{m}^3$ )	$\Omega$	$4.09 \times 10^{-29}$
Surface energy (inpore) ( $\text{J m}^{-2}$ )	$\gamma_s$	$0.41(0.85-1.4 \times 10^{-4}T)$ , with $0 < T < 2850^\circ\text{C}^a$
Surface diffusion coefficient ( $\text{m}^2 \text{s}^{-1}$ )	$D_s$	$50 \exp(-450000/RT)$
Layer thickness for surface diffusion (m)	$\delta_s$	$3 \times 10^{-10}$
Dihedral angle (inpore) (deg)	$\Psi$	$91.5^\circ$ <sup>a</sup>

<sup>a</sup> From a review by Hall and Mortimer [33].

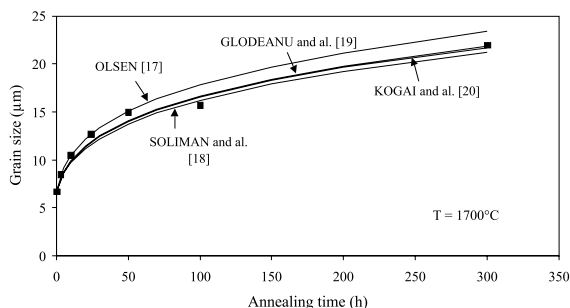


Fig. 6. Comparison between predicted change in grain size from published grain growth kinetics and experimental results (■) of Glodeanu et al. [19] at  $T = 1700^\circ\text{C}$ .

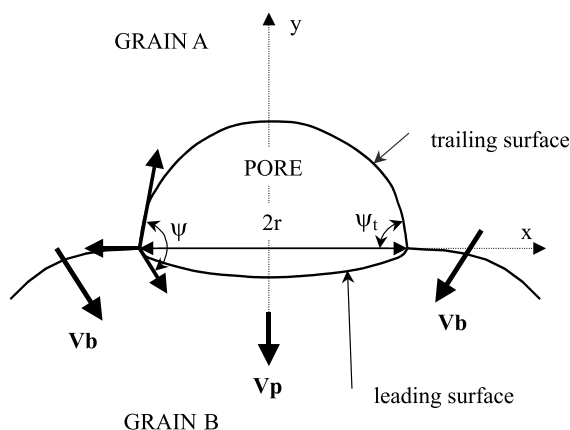


Fig. 7. Diagram of a moving pore, located on a two-grain interface, indicating the dihedral angles  $\psi$  and  $\psi_t$ .

to the driving mechanism are given in Fig. 7, with porosity consisting in two spherical caps.  $V_b$  indicates the migration rate of a grain boundary and  $V_p$  that of an intergranular pore.

Hsueh and Evans choose a value of  $\pi/2$  for the angle  $\psi_t$  as the approximate transition criterion between steady migration ( $V_p = V_b$ ) and unsteady migration ( $V_p < V_b$ ). Beyond  $\pi/2$ , the boundary bends inwards to reduce the contact length ( $2r$ ) and then to leave the pore behind. They were thus able to obtain maximum

migration rates in a steady state according to the active mechanism. These rates are established for conditions where the transport of matter by diffusion in the bulk is very low in relation to the two mechanisms considered:

#### EC migration

$$(V_p^{\text{EC}})_{\text{max}} = \frac{2\Omega\gamma_s}{kTr} \sqrt{\frac{2m}{\pi kT}} \frac{P_0}{\rho} (0.13\psi^2 - 0.85\psi + 1.4),$$

#### surface diffusion migration

$$(V_p^{D_s})_{\text{max}} = \frac{\Omega D_s \delta_s \gamma_s}{kTr^3} (17.9 - 6.2\psi),$$

with  $m$ ,  $\Omega$ : molar mass and volume of the material,  $P_0$ : saturation vapour pressure,  $\rho$ : density of material,  $D_s$ : surface diffusion coefficient,  $\gamma_s$ : solid–vapour surface energy in pores,  $\delta_s$ : layer thickness of the surface diffusion,  $r$ : contact radius (cf. Fig. 7),  $\Psi$ : dihedral angle ( $= \Psi_t + \Psi_l$ ), a geometrical invariant during migration.

In the case of  $\text{UO}_2$ , it is possible to compare these two rates, even though attention has again to be drawn to the strong influence of the  $O/U$  ratio of the condensed phase on these two mechanisms. The partial pressure of the  $\text{UO}_2$  ( $v$ ) above  $\text{UO}_{2.000}$  is calculated on the basis of the relationship proposed by Ackermann et al. [32]:

$$\log_{10} P(\text{UO}_2) = 67.531 + 4.382 \times 10^{-3} T - 4.411 \times 10^{-7} T^2 - 37090/T - 19.070 \log_{10} T$$

with  $P(\text{UO}_2)$  in atm and  $T$  in K.

As far as the surface diffusion coefficient is concerned, Eq. (6) established by Matzke was used. The thickness concerned by surface diffusion was fixed at a single layer that is about 3 Å. All the other parameters used are given in Table 4. The results of this computation are given in Fig. 8. It shows that pore migration rates can be increased by several orders of magnitude for the relatively narrow range of temperatures studied and that the surface diffusion mechanism predominates in the temperature range generally investigated for grain growth studies. At  $1700^\circ\text{C}$ , for example, surface diffusion provides higher rates than in vapour phase transport mode, for pore sizes below 20  $\mu\text{m}$ , and a transition in the rate controlling mechanism could be expected.



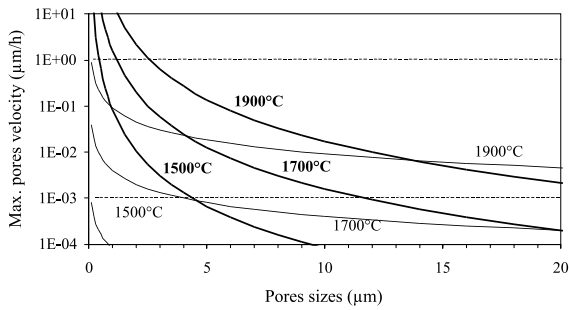


Fig. 8. Maximum pore velocity as a function of temperature and pore size in stoichiometric  $\text{UO}_2$ . The thick lines correspond to a surface diffusion pore movement mechanism, the thin ones to an EC pore movement mechanism.

All the numerical values obtained are subject to the uncertainty introduced by the hypotheses of the models used and the accuracy of certain parameters, particularly the surface diffusion coefficient. Nevertheless, it would seem that a correct order of magnitude for pore migration rates can be obtained by using the model established by Hsueh et al. For example, migration rates at  $1700^\circ\text{C}$  are too low above  $5\ \mu\text{m}$  to be significant, confirming the ability of the pores to slow down the boundaries motion. On the other hand, below  $5\ \mu\text{m}$ , migration rates increase rapidly, reaching several tens of  $\mu\text{m h}^{-1}$ , if the pores migrate by surface diffusion. Boundary migration rates being well below  $10\ \mu\text{m h}^{-1}$ , according to the kinetics recorded, it must be concluded that these pores have no marked boundary anchoring effect, as a slight deformation of their surface ensures sufficient flow for the pores to be able to migrate with the boundaries. In other words, these small pores will remain at the grains boundaries during grain growth. This location makes their elimination easy, thus providing a densification associated with the grain growth.

The critical pore size,  $2r_c$ , for which migration rates are the same for both mechanisms, has been established as a function of temperature:

$$(V_p^{\text{EC}})_{\text{max}} = (V_p^{D_s})_{\text{max}} \leftrightarrow 2r_c = 2 \times \left( \frac{D_s \delta_s \rho}{P_0} \sqrt{\frac{\pi k T}{2m}} \right)^{0.5} \times \left( \frac{17.9 - 6.2\psi}{0.13\psi^2 - 0.85\psi + 1.4} \right)^{0.5} \quad (8)$$

The corresponding curves are plotted in Fig. 9 for two values of  $D_s$  differing by a factor of 10 (standard deviation according to Matzke [24]). This figure also delineates the zones where the surface diffusion or EC mechanisms are the most efficient mechanisms of porosity migration, for stoichiometric  $\text{UO}_2$ .

For all sizes of residual sintering pores, surface diffusion seems to be the main migration mechanism. This predominance of surface diffusion for  $\text{UO}_2$  is in agree-

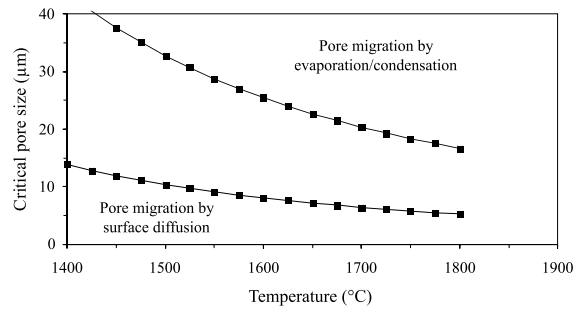


Fig. 9. Plots of the critical pore size ( $2r_c$ ) the separating surface diffusion mechanism from the EC mechanism, as a function of temperature.

ment with the results of Hsueh and Evans [31] in the case of alumina, where EC can be discounted as a significant mechanism for pores of reasonable size (less than  $20\ \mu\text{m}$ ). These results can be compared with those of Zhao and Harmer [29], who introduced 15 vol% of pore-forming agents graded at a few microns, into an alumina powder. A study of the final sintering stage, where these size controlled pores stayed on the boundaries, revealed that grain growth kinetics at  $T = 1850^\circ\text{C}$ , corresponded to a surface diffusion pore migration mechanism. For  $\text{MgO}$  EC is a more competitive mechanism than surface diffusion because of the high vapour pressures. However, for pores of  $1\ \mu\text{m}$ , vapour phase transport becomes predominant only at high temperatures, of the order of  $2100^\circ\text{C}$  [31]. Thus  $\text{UO}_2$  presents characteristics, which are intermediate between alumina on one side and magnesia on the other, for which vapour pressures are relatively high.

## 7. Conclusions

Grain growth and density increase of  $\text{UO}_2$  has been measured during annealings at temperatures between  $1650^\circ\text{C}$  and  $1750^\circ\text{C}$ , for up to 300 h. The results have been compared to what can be deduced from a review of grain growth kinetics for undoped uranium dioxide. Grain boundary pinning by the pores is expected to control the kinetics of grain growth, but the precise mechanism of the pore migration remain uncertain, and will not be obtained simply by studying the grain growth kinetics of undoped  $\text{UO}_2$ .

A number of limitations concerning data analysis have been identified. Even disregarding the wide variations in activation energies of the pore migration mechanisms with the exact O/U ratio in the condensed phase, the methods used to obtain the grain growth kinetic parameters  $n$ ,  $k_0$  and  $Q$  are such that the experimental value of the activation energy  $Q$  cannot be given with any certainty. The relationships obtained reflect

more the choice of a better fitting of experimental points rather than physical quantities.

The analysis of pore migration rates shows that surface diffusion predominates over EC as a transport mode for ordinary pore sizes. However, these results depend to a great extent on the reliability of surface diffusion data obtained through mass transport methods.

### Acknowledgements

The authors would like to thank FRAMATOME, without whose support this study would not have been possible. The authors also wish to thank Mr A. Hammou, professor at Joseph Fourier University of Grenoble, Mr J.F. Baumard, professor at the Ecole Nationale Supérieure de Céramiques Industrielles, Limoges, who supervised the thesis work carried out by Mr L. Bourgeois. This work was achieved in the Laboratoire de Radiométaballurgie des Combustibles du Département de Thermohydraulique et de Physique.

### References

- [1] J.A. Turnbull, *J. Nucl. Mater.* 50 (1974) 62.
- [2] P.T. Sawbridge, J.C. Killeen, CEGB Report RD/B/N 4866, 1980.
- [3] P.T. Sawbridge, C. Baker, R.H. Cornell, K.W. Jones, D. Reed, *J. Nucl. Mater.* 95 (1980) 119.
- [4] J.E. Burke, D. Turnbull, *Prog. Met. Phys.* 3 (1952) 220.
- [5] M.P. Anderson, D.J. Srolovitz, G.S. Grest, P.S. Sahni, *Acta Metall.* 32 (1984) 783.
- [6] W.D. Kingery, B. Francois, *J. Am. Ceram. Soc.* 48 (1965) 546.
- [7] F.A. Nichols, *J. Appl. Phys.* 37 (1966) 4599.
- [8] R.J. Brook, in: F.F.Y. Waing (Ed.), *Treatise Materials Science Technology, Ceramics*, vol. 9, Academic Press, New York, 1979, p. 331.
- [9] D.J. Srolovitz, M.P. Anderson, G.S. Grest, P.S. Sahni, *Scr. Metall.* 17 (1983) 241.
- [10] D.J. Srolovitz, M.P. Anderson, P.S. Sahni, G.S. Grest, *Acta Metall.* 32 (1984) 793.
- [11] J.R. MacEwan, J. Hayashi, *Proc. Br. Ceram. Soc.* 7 (1965) 245.
- [12] J.E. Burke, *Trans. AIME* 180 (1949) 73.
- [13] J.B. Ainscough, B.W. Oldfield, J.O. Ware, *J. Nucl. Mater.* 49 (1973/1974) 117.
- [14] J.R. MacEwan, *J. Am. Ceram. Soc.* 45 (1962) 37.
- [15] M.F. Lyons, D.H. Coplin, B. Weidenbaum, EURAEC Report GEAP-4411, 1963.
- [16] D. Weygand, Y. Brechet, J. Lepinoux, *Acta Mater.* 46 (1998) 6559.
- [17] C.S. Olsen, in: *Structural Mechanisms in Reactor Technology, Trans., Analysis of Reactor Fuel and Cladding Materials*, vol. C, North-Holland, Amsterdam, NL, 1979, p. C1/9 (1–10).
- [18] S.E. Soliman, N. Hansen, I. Misfeldt, J.G. Rasmussen, T. Sorensen, in: Hansen (Ed.), *Proceedings of the Seventh RISØE International Symposium on Metallurgy and Materials Sciences*, September 1986, Risø National Laboratory, Roskilde, Denmark.
- [19] F. Glodeanu, I. Furtuna, A. Paraschiv, M. Paraschiv, *J. Nucl. Mater.* 148 (1987) 351.
- [20] T. Kogai, R. Isawaki, M. Hirai, *J. Nucl. Sci. Technol.* 26 (1989) 744.
- [21] Ch. Younes, PhD thesis, Université de Paris-Sud, Orsay, France, vol. 3199, 1986.
- [22] D.B. Knorr, R.M. Cannon, R.L. Coble, *Acta Metall.* 8 (1989) 2103.
- [23] P.S. Maiya, *J. Nucl. Mater.* 40 (1971) 57.
- [24] H.J. Matzke, in: L.C. Dufour, J. Nowotny (Eds.), *Surfaces and Interfaces of Ceramics Materials*, Kluwer Academic, Dordrecht, 1989, p. 241.
- [25] D.R. Olander, *J. Nucl. Mater.* 96 (1981) 243.
- [26] M.O. Marlowe, A.I. Kazanoff, *J. Nucl. Mater.* 25 (1968) 328.
- [27] S.Y. Zhou, D.R. Olander, *Surf. Sci.* 136 (1984) 82.
- [28] H.J. Matzke, in: *Proceedings of the Fifth International Conference on Plutonium and Others Actinides*, 1975, Baden-Baden, Germany, North-Holland, Amsterdam, 1976, p. 801.
- [29] J. Zhao, M.P. Harmer, *J. Am. Ceram. Soc.* 75 (1992) 830.
- [30] C.H. Hsueh, A.G. Evans, R.L. Coble, *Acta Metall.* 30 (1982) 1269.
- [31] C.H. Hsueh, A.G. Evans, *Acta Metall.* 31 (1983) 189.
- [32] R.J. Ackermann, E.G. Rauh, M.H. Rand, in: *Proceedings of the International Symposium of Thermodynamics of Nuclear Materials*, IAEA, Jülich, 1979.
- [33] R.O.A. Hall, M.J. Mortimer, *J. Nucl. Mater.* 148 (1987) 237.
- [34] R.N. Singh, *J. Nucl. Mater.* 64 (1977) 174.